# Investigating the low frequency content of the Hussar data with impedance inversion

Heather J.E. Lloyd and Gary F. Margrave

## ABSTRACT

Acoustic impedance inversion can easily be computed by the BLIMP (BandLimited IMPedance) algorithm. This algorithm uses well logs to fill in the low-frequency information that is missing in bandlimited seismic data. The transition from well log low-frequency information to the seismic data spectrum is marked by a cut-off frequency, $f_c$. The choice of $f_c$ depends on the low-frequency content of the seismic data, and it is generally desirable to push $f_c$ as low as possible to make the inversion less dependent on well control. For the Hussar data, with 10 Hz geophones and dynamite sources, an $f_c$ as low as 2 Hz gives good results. This is relatively low compared to the 5 to 10 Hz that is commonly chosen for most seismic data. Three wells intersect the Hussar line and all were used to calculate inversions as well as a well log that was prepared by averaging the three impedance logs. The average log was found to produce the best inversions with a mean impedance error of 8.5% from .2 to 1.05 seconds, where wells 12-27, 14-27 and 14-35 produced errors of 11%, 10% and 10% respectively over the same interval. Other cut-off frequencies were also examined and the best choice appears to be non-stationary, as frequencies down to 1.5 Hz can be trusted in the shallower section. This study has shown that the Hussar data set has trusted frequencies down to 1.5 - 2 Hz.

## INTRODUCTION

Final seismic sections present an estimate of reflectivity, which is an interface property; however, an acoustic impedance inversion of the reflectivity estimate makes impedance, an inherent rock property, available for analysis. From impedance the velocity, density and other rock properties can be derived. Depth conversion is also possible using the calculated velocities from impedance (Lindseth 1979). Simple acoustic impedance inversions can be computed using the BLIMP (BandLimited IMPedance) algorithm (Ferguson and Margrave, 1996). This method uses the following steps to compute the inversion:

1. Compute the linear trend of the impedance log and remove it to help reduce edge effects introduced during Fourier domain calculations.
2. Compute the Fourier spectrum of the modified impedance log.
3. Apply a bandlimited integration filter to the seismic trace and then exponentiate the result of the filter. The bandlimited integration filter`s limits are selected by the user.
4. Compute the Fourier spectrum of the integrated and exponentiated seismic trace (3).
5. Determine a scalar that matches the mean power from the spectrum of the impedance log (2) to the spectrum of the integrated seismic trace (4).
6. Multiply the spectrum of the integrated seismic trace by the scalar determined in (5).

7. Apply a low-pass filter to the impedance log spectrum (2) and add to the scaled seismic spectrum (6). The low pass value is called the low-frequency cut-off, $f_c$, and is selected by the user.
8. Inverse Fourier Transform the result in (7).
9. Add the linear trend that was removed in (1) to generate the completed impedance result.

To compute an accurate inversion the low-frequency cut-off must be chosen with care. If the cut-off is too low, low-frequency noise from the seismic data will contaminate the inversion. If the cut-off is too high, the inversion is overwhelmed by well information and subtle details from the seismic data cannot be seen. The well impedance log that is chosen for the inversion is also important. Ideally this log needs to contain a similar trend (i.e. low frequency information) as the other wells in the area.

In this study the Hussar data set will be used. It was collected using 10 Hz geophones and a dynamite source so it should contain very low frequency information. It was processed by CGGVeritas with care taken to preserve the low frequency signal. This data was then conditioned as described in Lloyd and Margrave 2012.

## METHOD

The well ties and balanced seismic data are shown in Figure 1. Once the data has been conditioned, we can begin to calculate the acoustic impedance inversions. To do this we use the BLIMP algorithm that combines the low frequencies of a well with the seismic data to produce an impedance inversion. The transition from low-frequency well information to the seismic data spectrum is controlled by a choice of cut-off frequency $f_c$. Ideally $f_c$ should be as low as possible so that most of the inversion is determined by the seismic data; but some well information, usually just a trend, is always required. Figures 3, 4 and 5 show the cut-off frequency tests where the low frequencies are added from wells 12-27, 14-27 and 14-35 respectively. In these Figures, a single seismic trace adjacent to the well is being inverted with various cut-off frequencies. To determine how close the inversions are approaching the well impedances a reference filtered impedance trace that is entirely from the well is plotted in the very right and left columns that are separated by a dashed line from the rest of the impedances. This filtered impedance comes from the respective well and has been filtered using the matching filter shown in Figure 2.

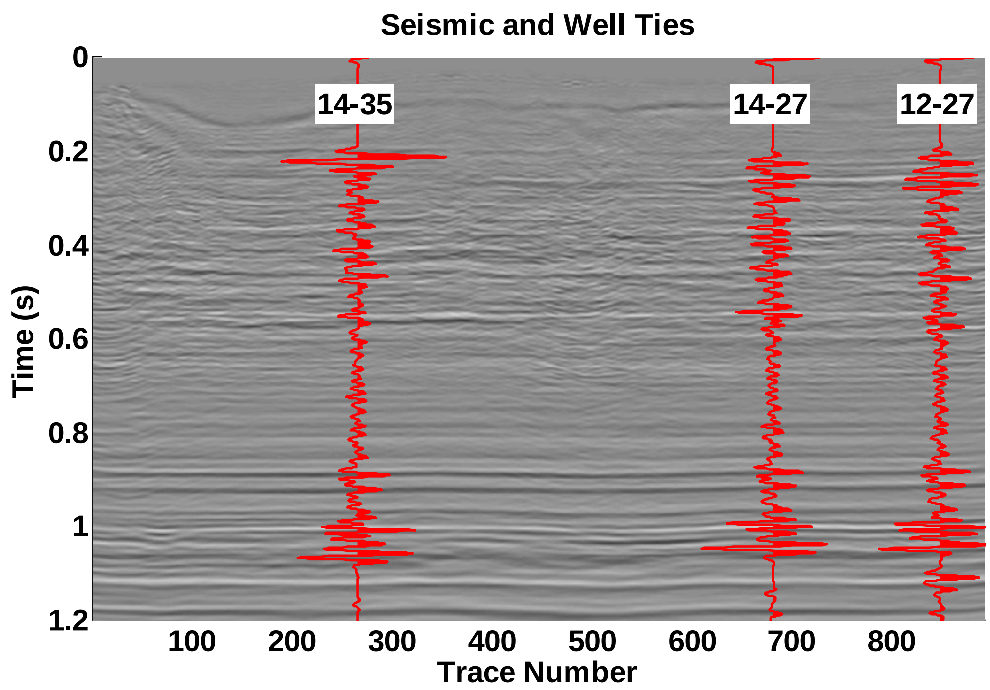


FIG 1: Seismic data and well ties for the dynamite and 10Hz geophones after migration and well ties.

The impedance inversions using wells 14-27 and 14-35 seem to stabilize between 2 and 3 Hz whereas the impedance inversion using well 12-27 seems to take longer. To evaluate the cut-offs more numerically Figure 6 shows the difference between adjacent inversion columns. From this plot we estimate that the lowest signal frequency to use is 2 Hz. However, lower frequencies still produce plausible results. This cut-off will be used when inverting the seismic sections. Further investigation of the low frequency cut-off will be discussed in the following section of this paper.

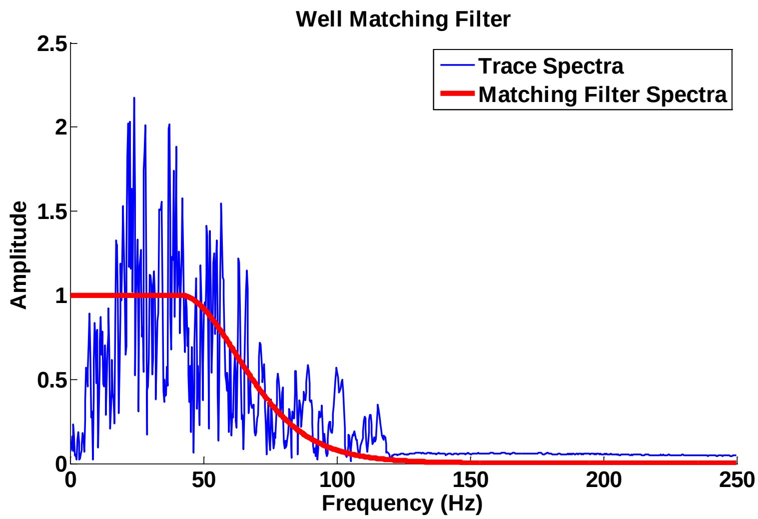


FIG 2: The filter that was used to attenuate the high frequencies of the Well impedance. This filter was used for all wells.

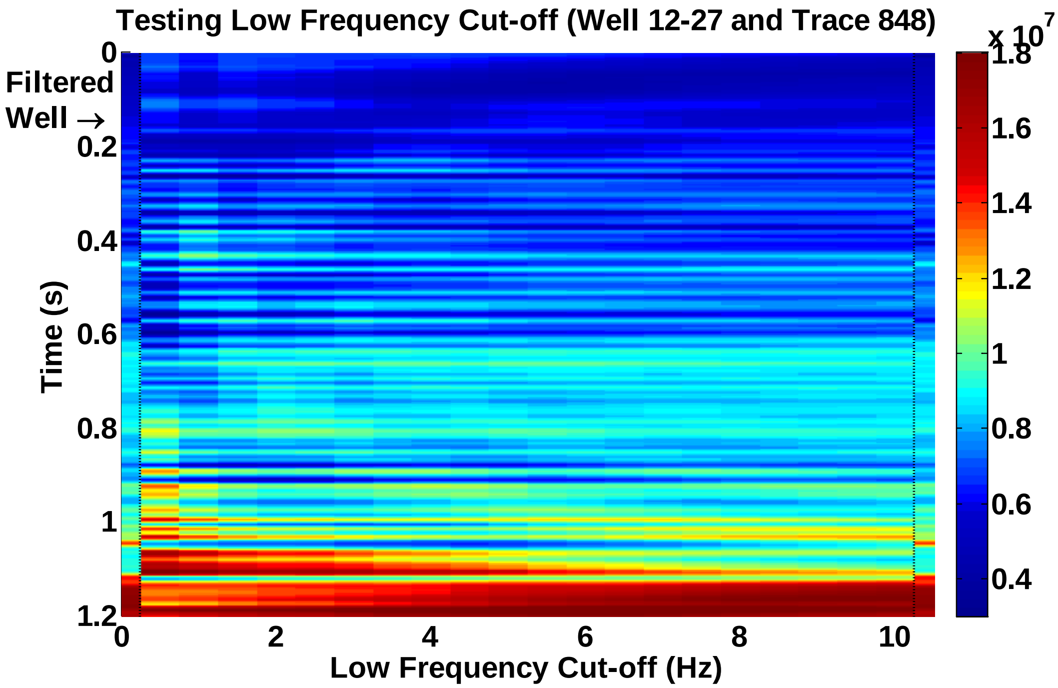


FIG 3: Frequency test to determine the best low frequency cut-off when using the impedance log from well 12-27. For comparison the filter impedance from well 12-27 is shown at the very right and left of the section.

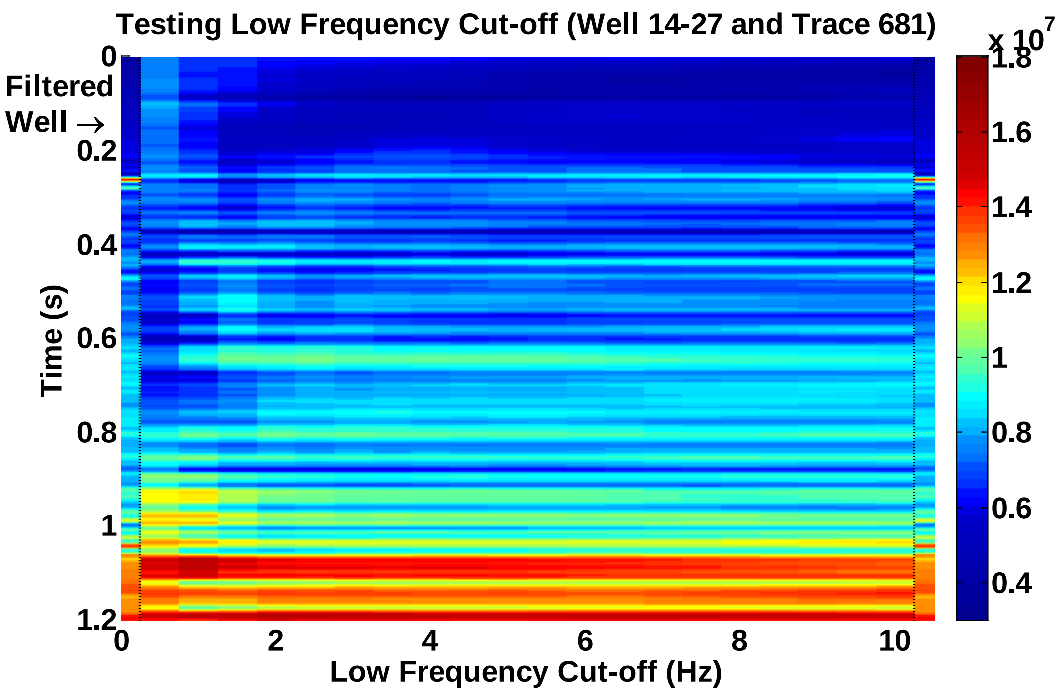


FIG 4: Frequency test to determine the best low frequency cut-off when using the impedance log from well 14-27. For comparison the filter impedance from well 14-27 is shown at the very right and left of the section.

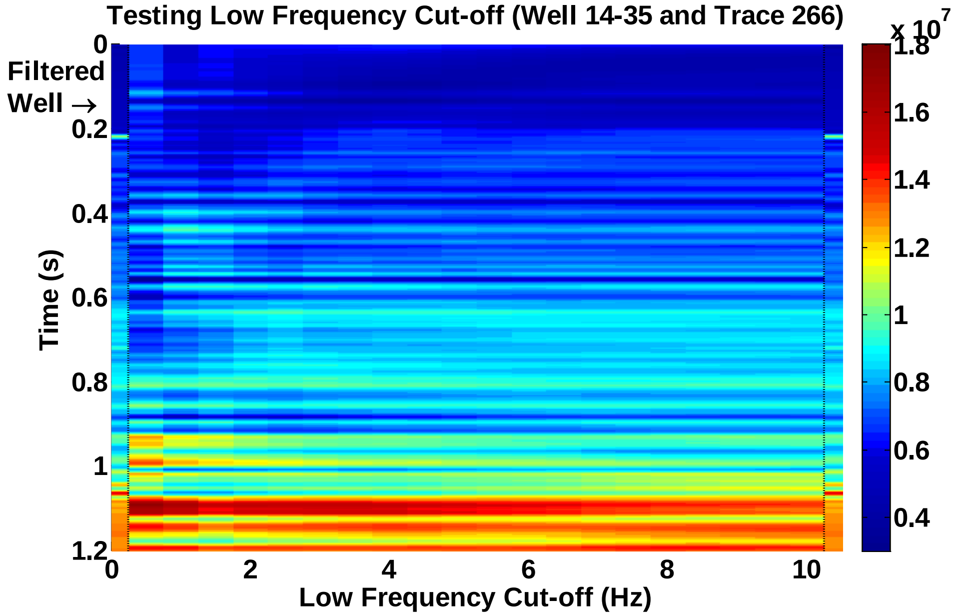


FIG 5: Frequency test to determine the best low frequency cut-off when using the impedance log from well 14-35. For comparison the filter impedance from well 14-35 is shown at the very right and left of the section.

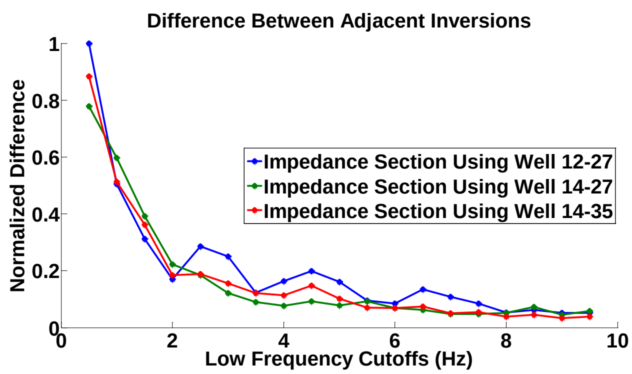


FIG 6: The normalized difference between adjacent inversions. Inversion stability is found when the low-frequency cut-off is at least 2 Hz.

Now that a suitable low-frequency cut-off has been found we can calculate the impedance sections. Figure 7 shows the impedance section calculated using low frequencies from well 12-27. A cross validation test was performed to ensure that the impedance inversions are suitable at the other well locations along the line. Figure 8 compares the inversion at each well location to the filtered well impedance logs using the matching filter in Figure 2. Visually the inversion does very well in matching the filtered well impedance especially in the reservoir area (0.8-1.1 seconds). The worst fit is in the underburden. Since the "well" information in this case came from the stacking velocities they will be ignored for now but a new underburden will eventually need to be computed that produces better results.

This process was repeated using well 14-27, Figures 9 and 10, and well 14-35, Figures 11 and 12. Similar results were found with each well. The average well impedance described in Lloyd and Margrave (2012) was also used and its results can be found in Figures 13 and 14.

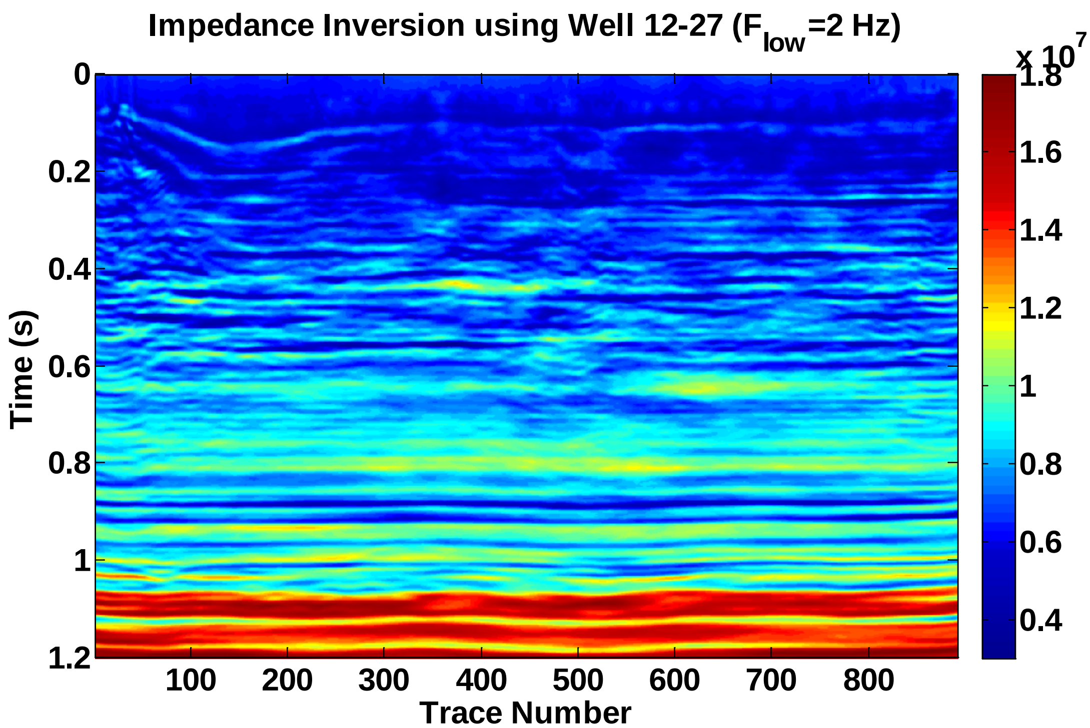


FIG 7: Impedance inversion calculated using well 12-27 and a low frequency cut-off of 2 Hz.

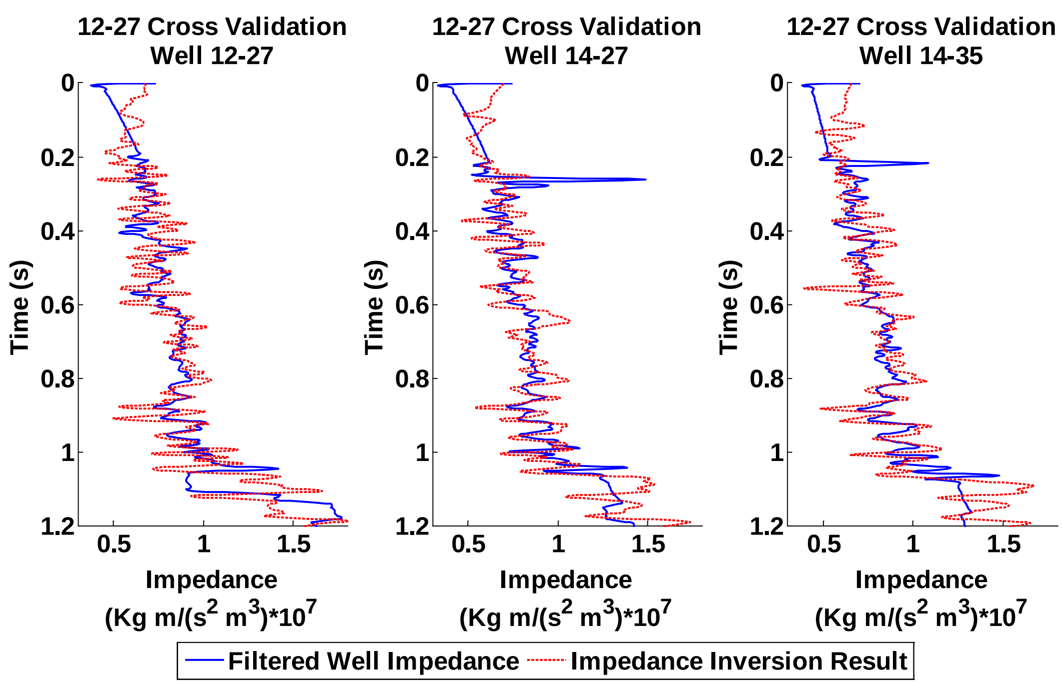


FIG 8: Cross validation plot that compares the inversion calculated using the impedance log from well 12-27 with the filtered well impedances.

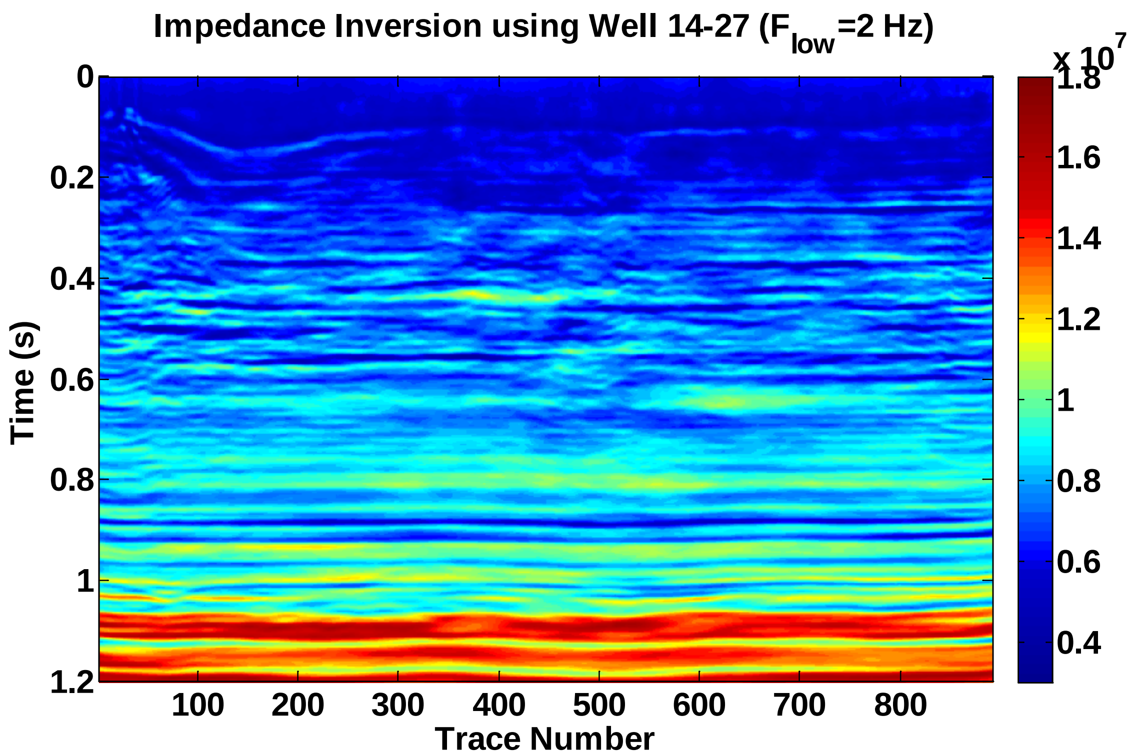


FIG 9: Impedance inversion calculated using well 14-27 and a low-frequency cut-off of 2 Hz.

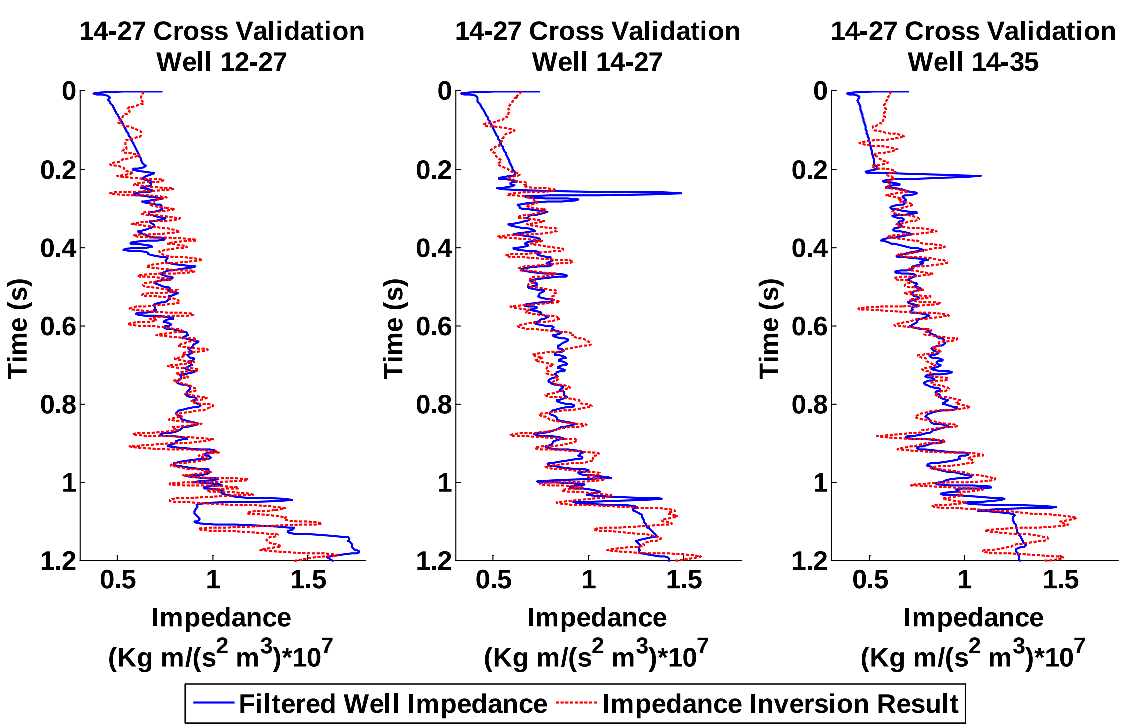


FIG 10: Cross validation plot that compares the inversion calculated using well 14-27 with the filtered well impedances.

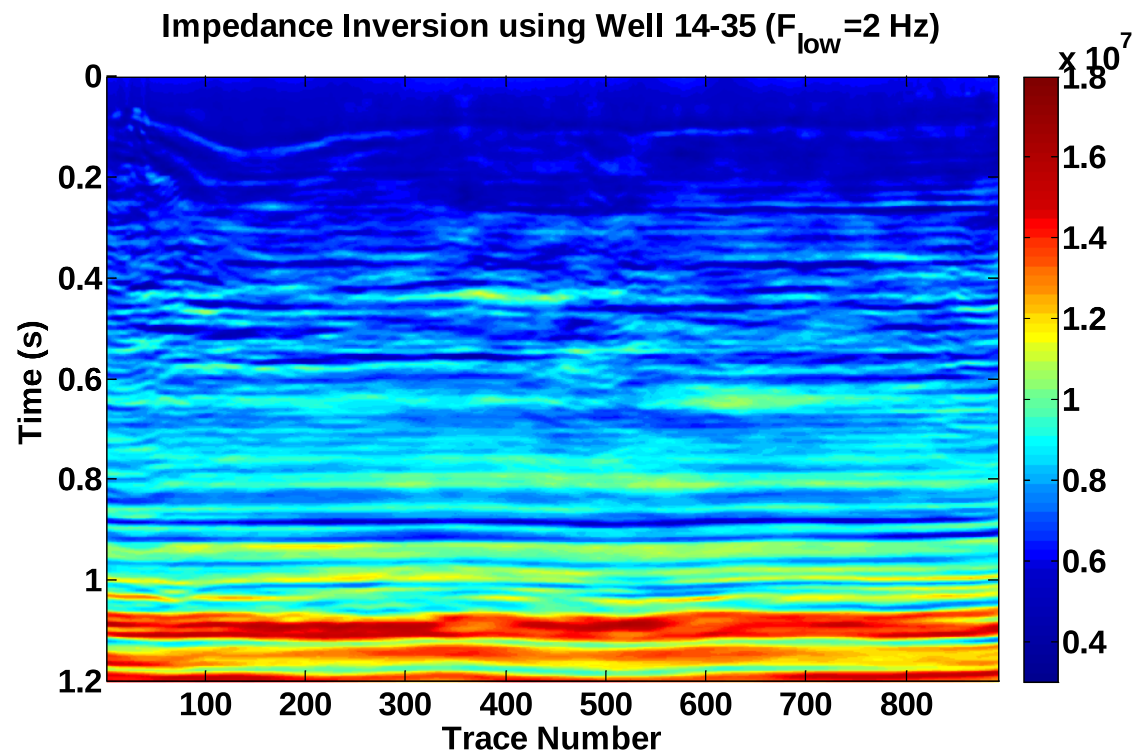


FIG 11: Impedance inversion calculated using well 14-35 and a low-frequency cut-off of 2 Hz.

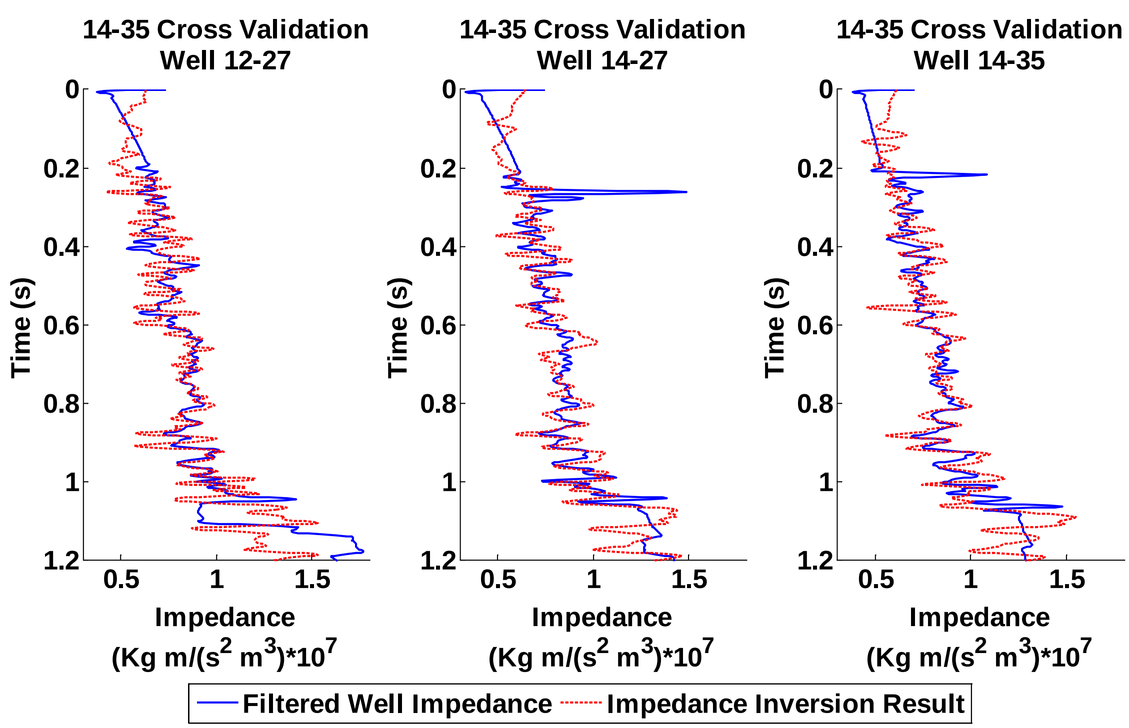


FIG 12: Cross validation plot that compares the inversion calculated using the impedance log from well 14-35 with the filtered well impedances.

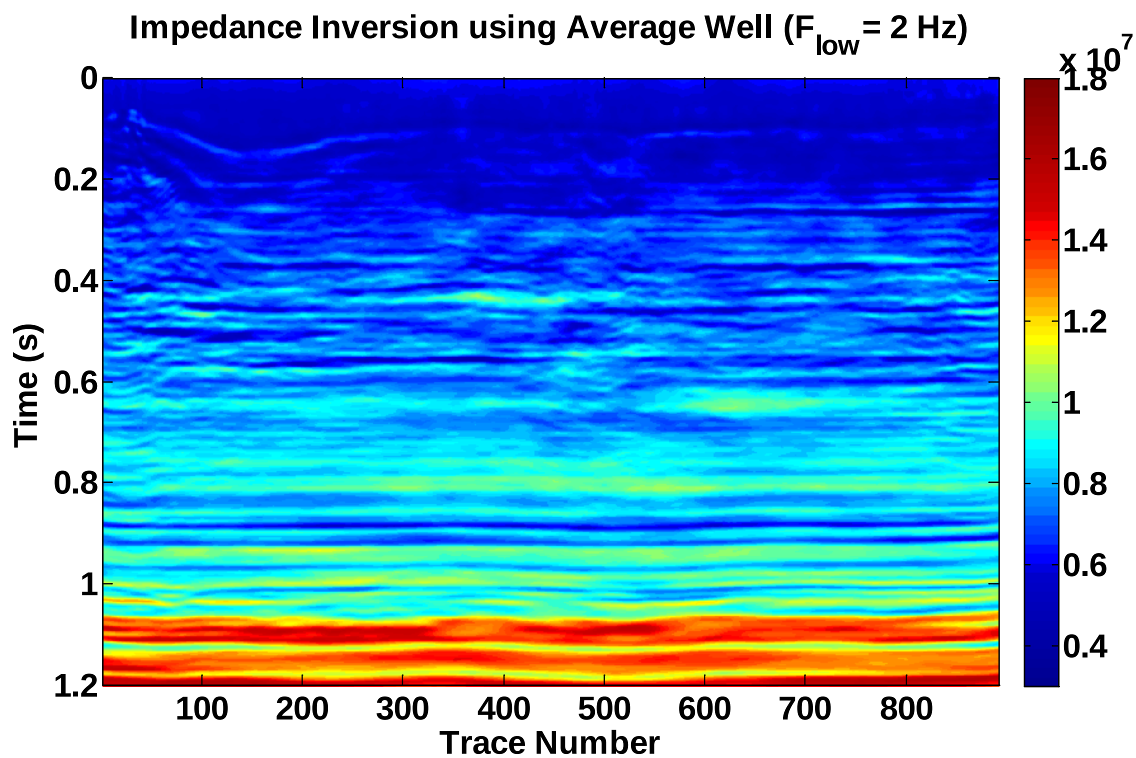


FIG 13: Impedance inversion calculated using the average well and a low-frequency cut-off of 2 Hz.

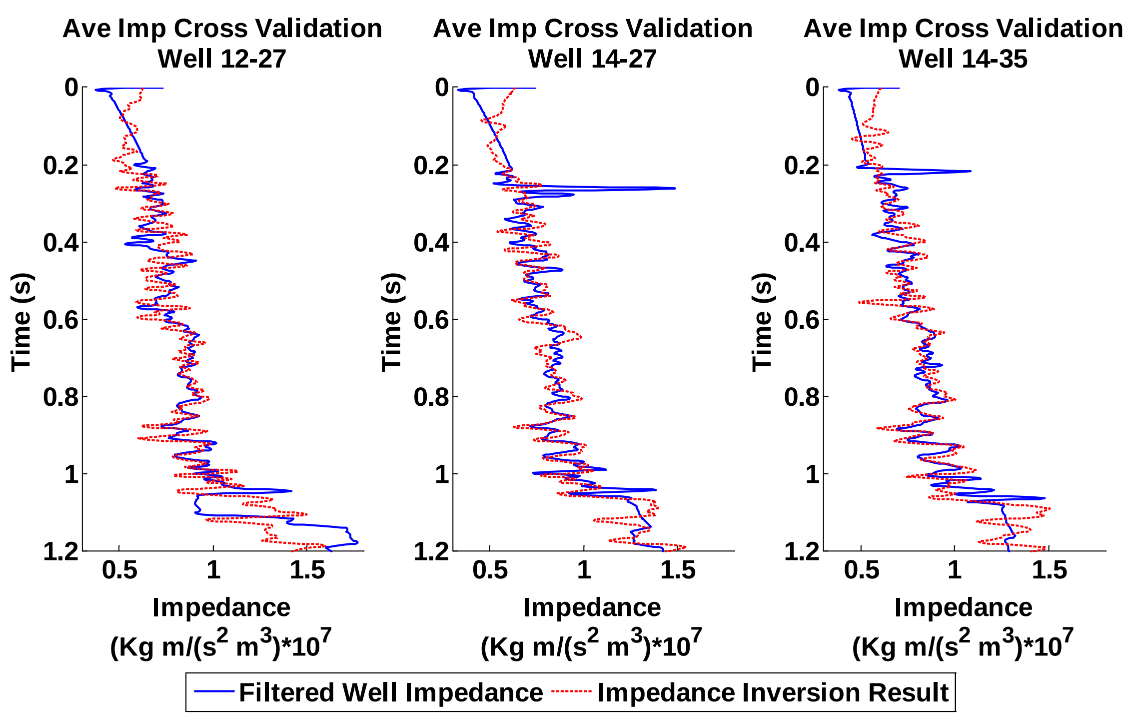


FIG 14: Cross validation plot that compares the inversion calculated using the impedance log from the average well with the filtered well impedances.

The percent difference between the filtered well and the inversions were calculated and displayed in Figure 15. On the far right panel is the cross validation percent error between the filtered impedance log from well 12-27 and the inversion results using well 12-27 (I1227), well 14-27 (I1427), well 14-35(I1435) and the average well (IMean). The other panels show the cross validation percent error between the filtered impedance log from well 14-27 and the inversion results, and the cross validation percent error between well 14-35 and the various inversions. The mean percent errors are shown above each column and are calculated in the interval from .2 to 1.05 seconds. For each case well 12-27 produces the worst results whereas the average well produces the results with the least error. Wells 14-27 and 14-35 produce very similar results between the two.

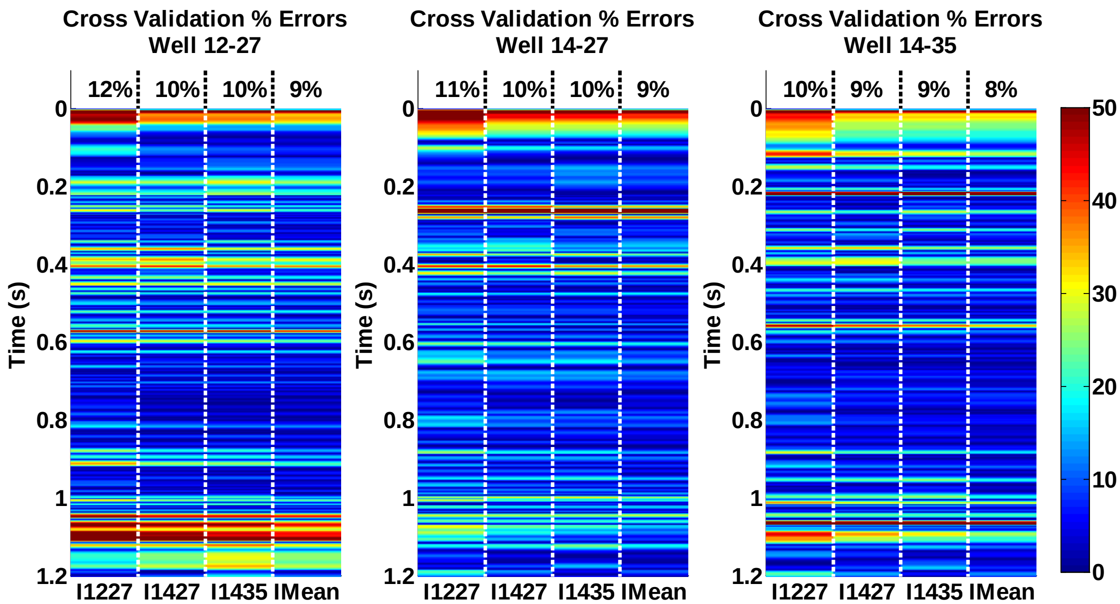


FIG 15: The cross validation percent errors from each impedance inversion when compared to the filtered impedance from each well. The number at the top of each error curve is the mean percent error calculated from .2 to 1.05 seconds.

## LOW-FREQUENCY INVESTIGATION

In Isaac et al. (2012) the phase coherence in the CGG Veritas processed hussar data contained phase coherence as low as 1 to 5 Hz. This suggests that there is signal in the data as low as 1 Hz. The using the difference in impedance for different low-frequency cut-offs has given that the lowest stable frequency is 2 Hz. Several cross validation tests were computed using low-frequency cut-offs of .5, 1, 1.5, 2, 2.5, 3 and 10 Hz, Figures 16 to 22 respectively. These tests were created using the average well log as the source for the low frequencies, the error was calculated between .2 to 1.05 seconds to avoid the overburden and underburden errors. For the low-frequency cut-off of 0.5 Hz, we can see that the inversion is not very stable especially in the 0.5 to 0.8 second range. This interval decreases from 0.6 to 0.8 seconds using a low-frequency cut-off at 1Hz. Once we get to 1.5 Hz though, the inversion is quite stable. It could be noted that there may be significant low-frequencies down to 1.5 Hz in the data. For low-frequency cut-offs from 2 to 3 Hz the inversion is quite stable with very little change in character and percent error. The 10Hz section has the least amount of error and the best fit however Figure 23 (bottom right hand panel) shows that this section is overly smoothed and highly influenced by the well. Any fluid changes or lithologies have been smoothed over. The Upper left hand panel in Figure 23 shows the inversion section using 0.5 Hz and while some events are continuous the impedance values seem to be much patchier especially in the reservoir interval from .8 to 1.1 seconds. The 1.5 Hz section, also shown in Figure 23, is very similar to the 2.0 Hz section providing more evidence that there is coherent data at 1.5 Hz.

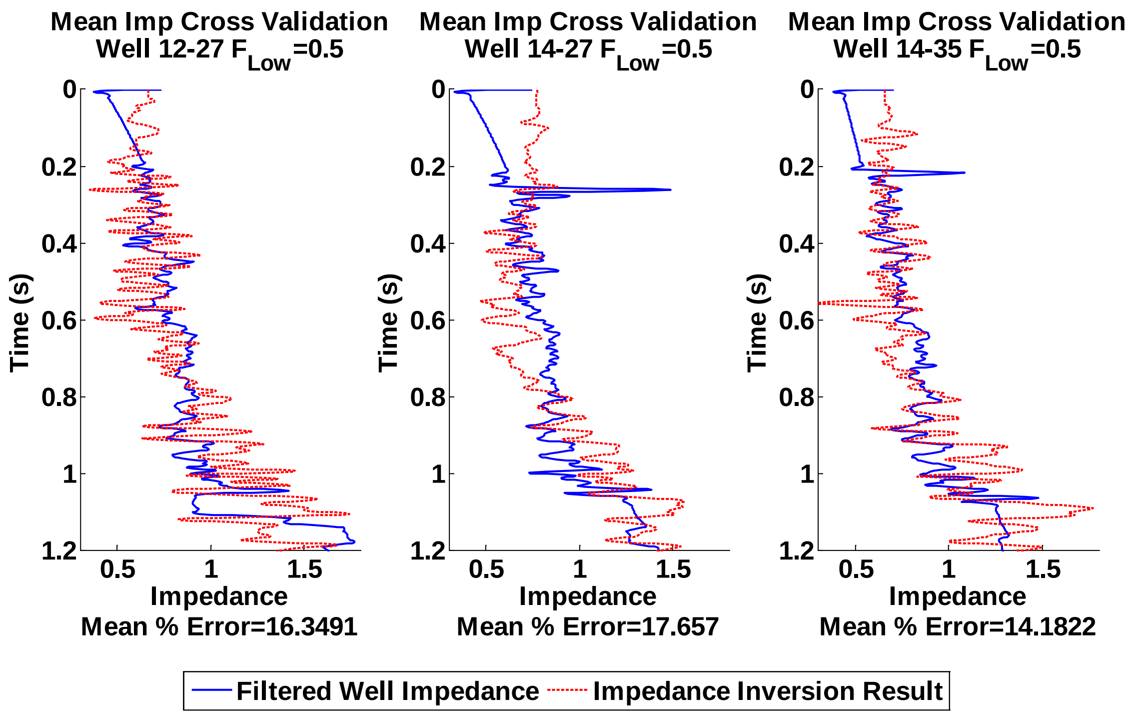


FIG 16: Cross-validation test using a low-frequency cut-off of 0.5 Hz

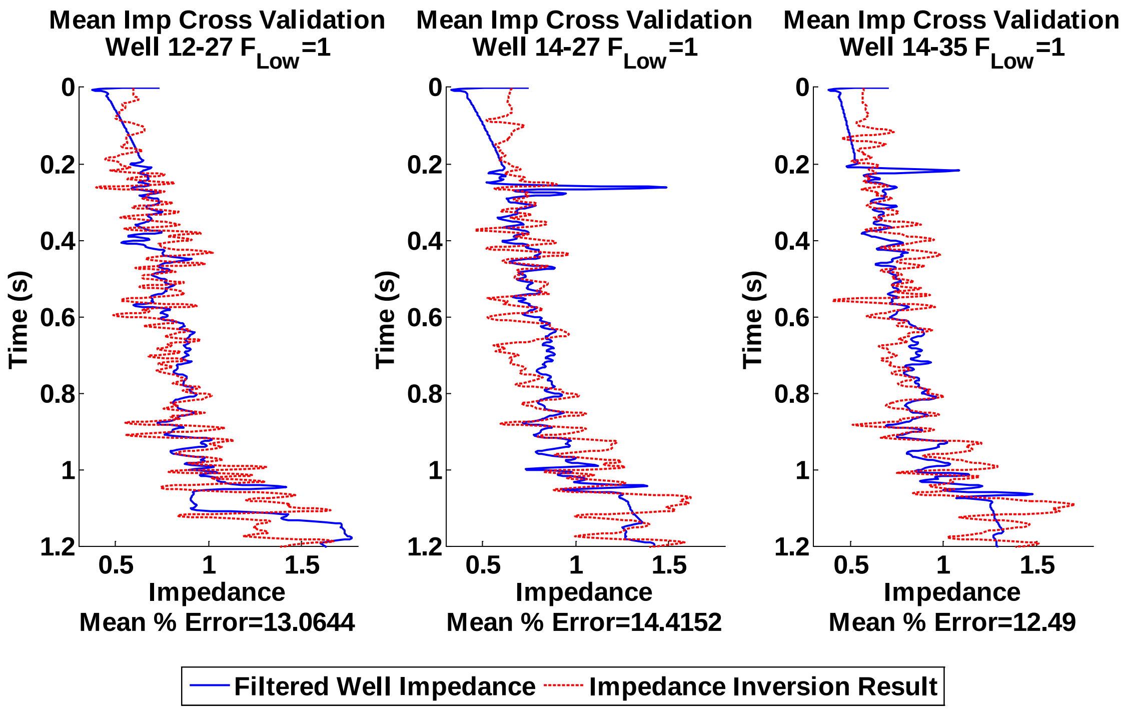


FIG 17: Cross-validation test using a low-frequency cut-off of 1Hz

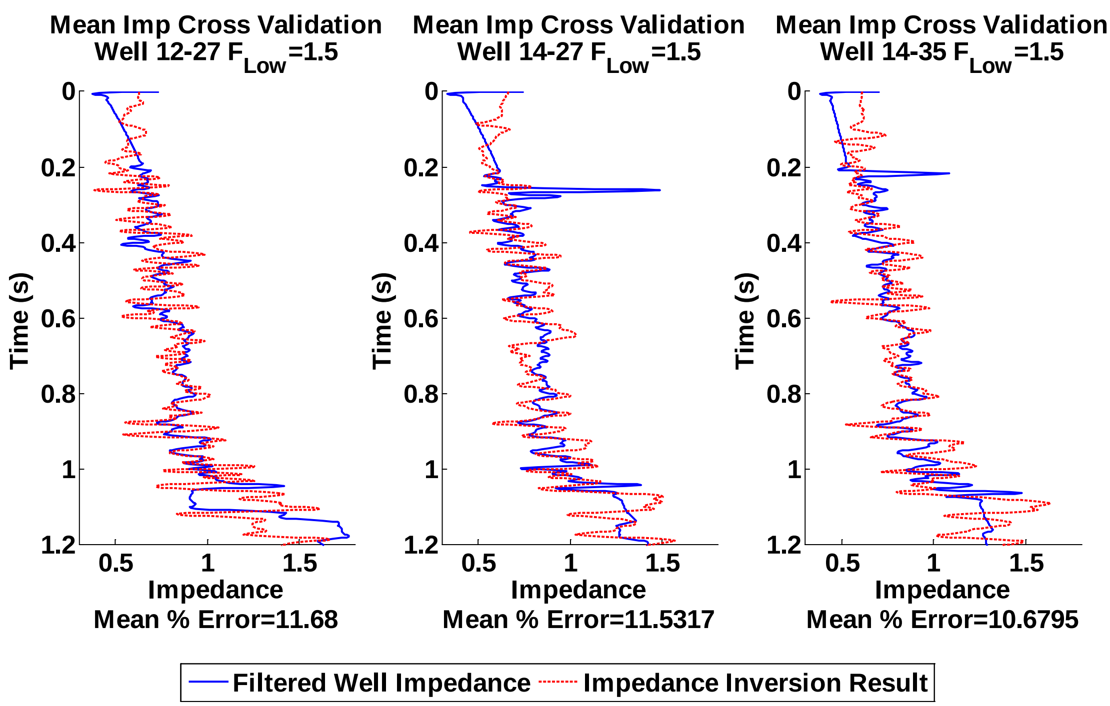


FIG 18: Cross-validation test using a low-frequency cut-off of 1.5 Hz

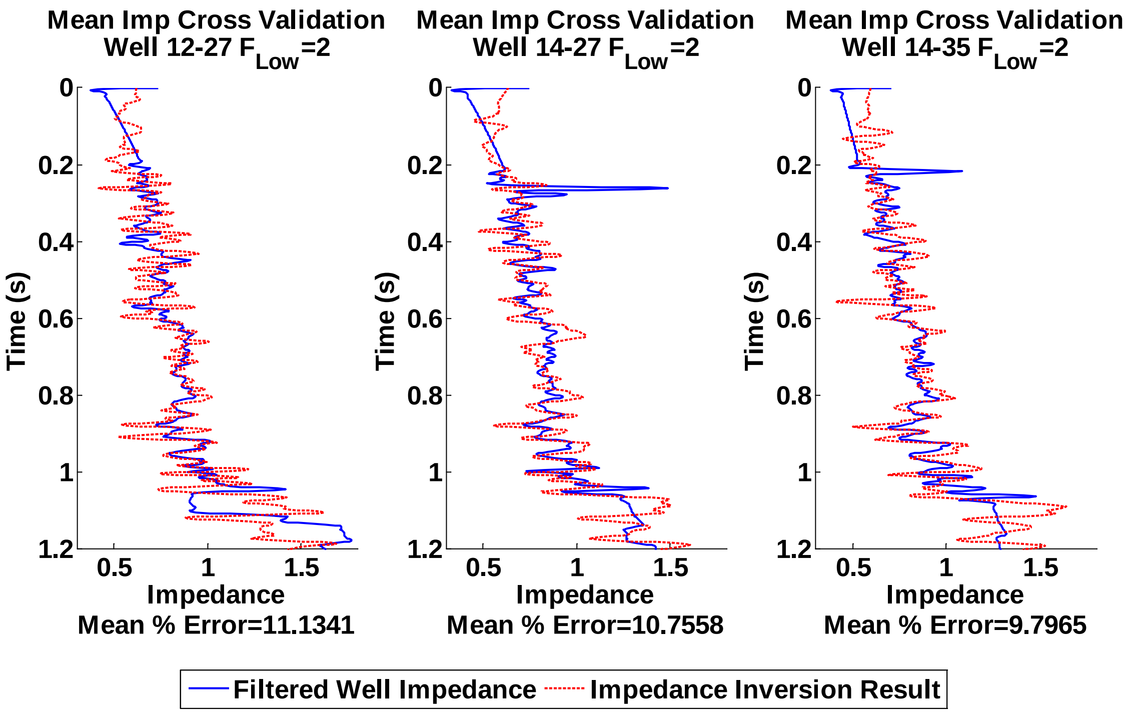


FIG 19: Cross-validation test using a low-frequency cut-off of 2 Hz

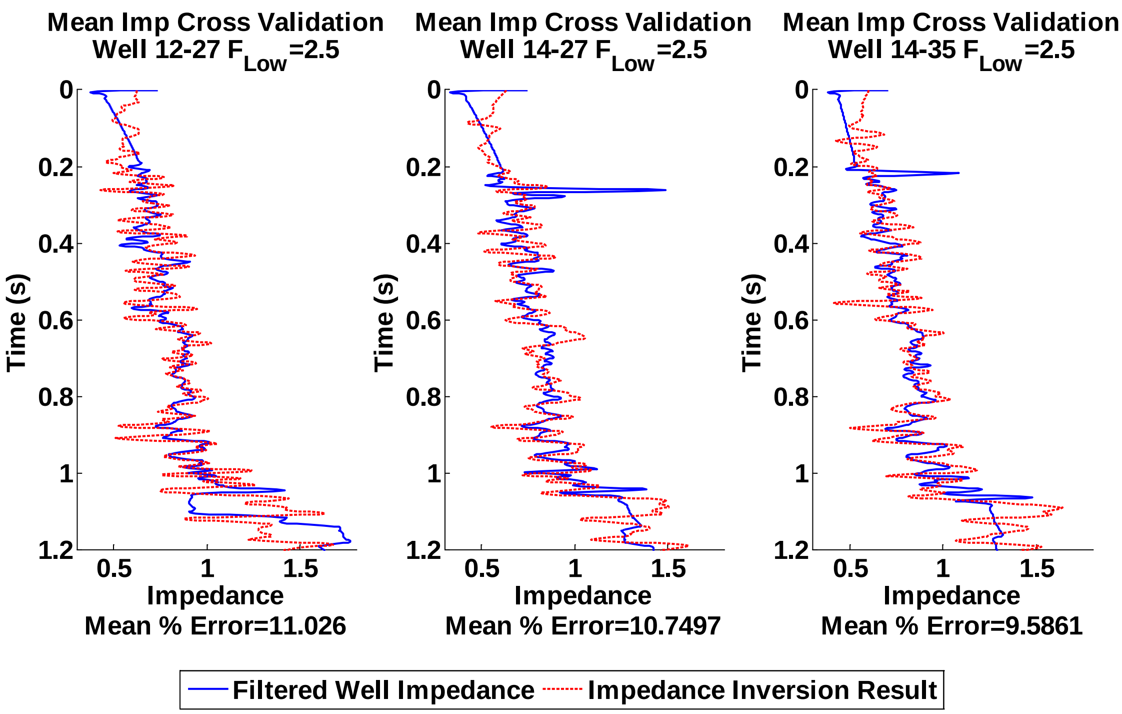


FIG 20: Cross-validation test using a low-frequency cut-off of 2.5 Hz

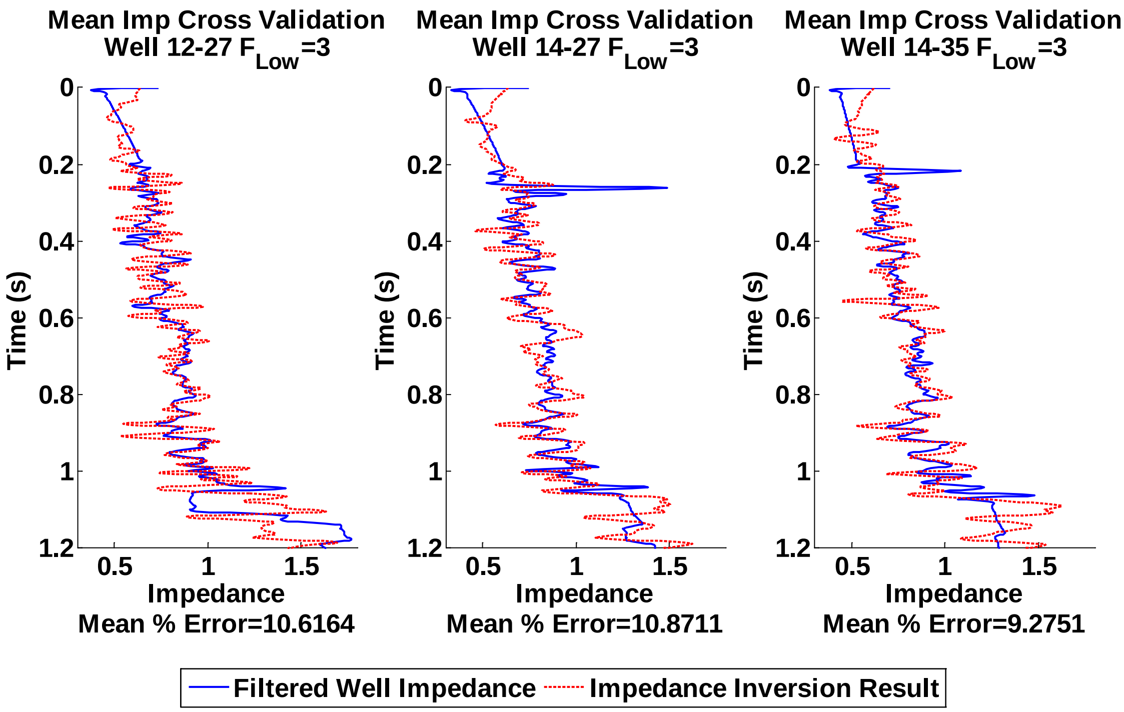


FIG 21: Cross-validation test using a low-frequency cut-off of 3 Hz

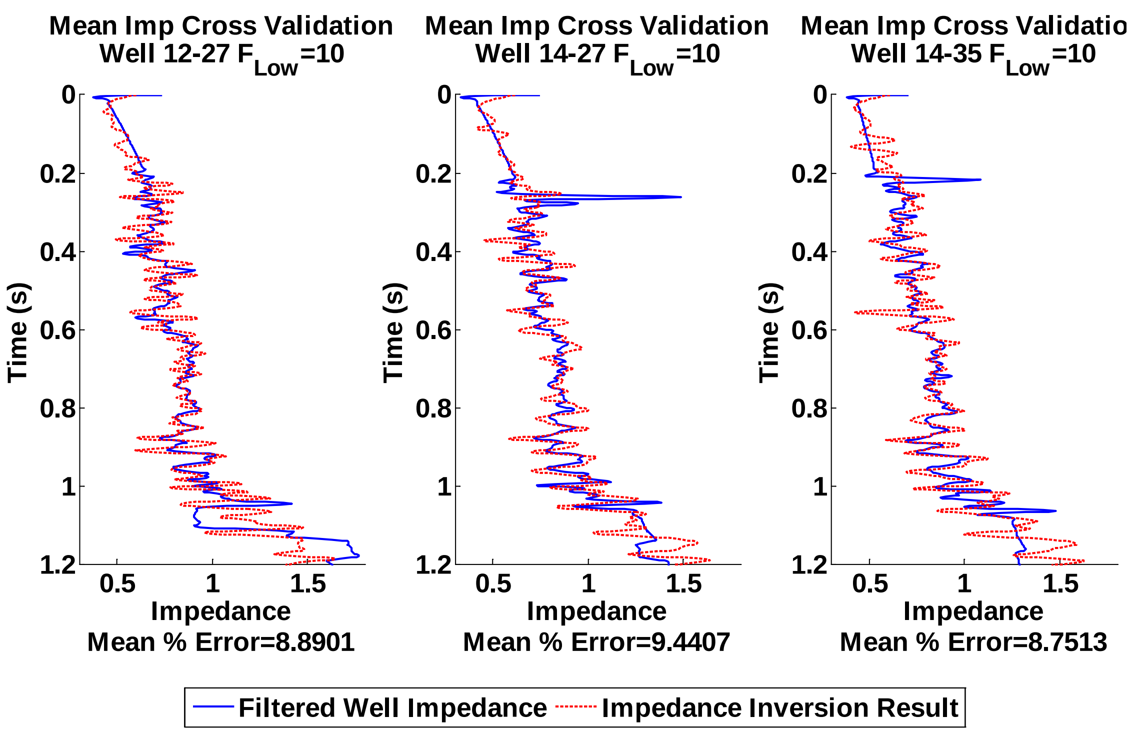


FIG 22: Cross-validation test using a low-frequency cut-off of 10 Hz

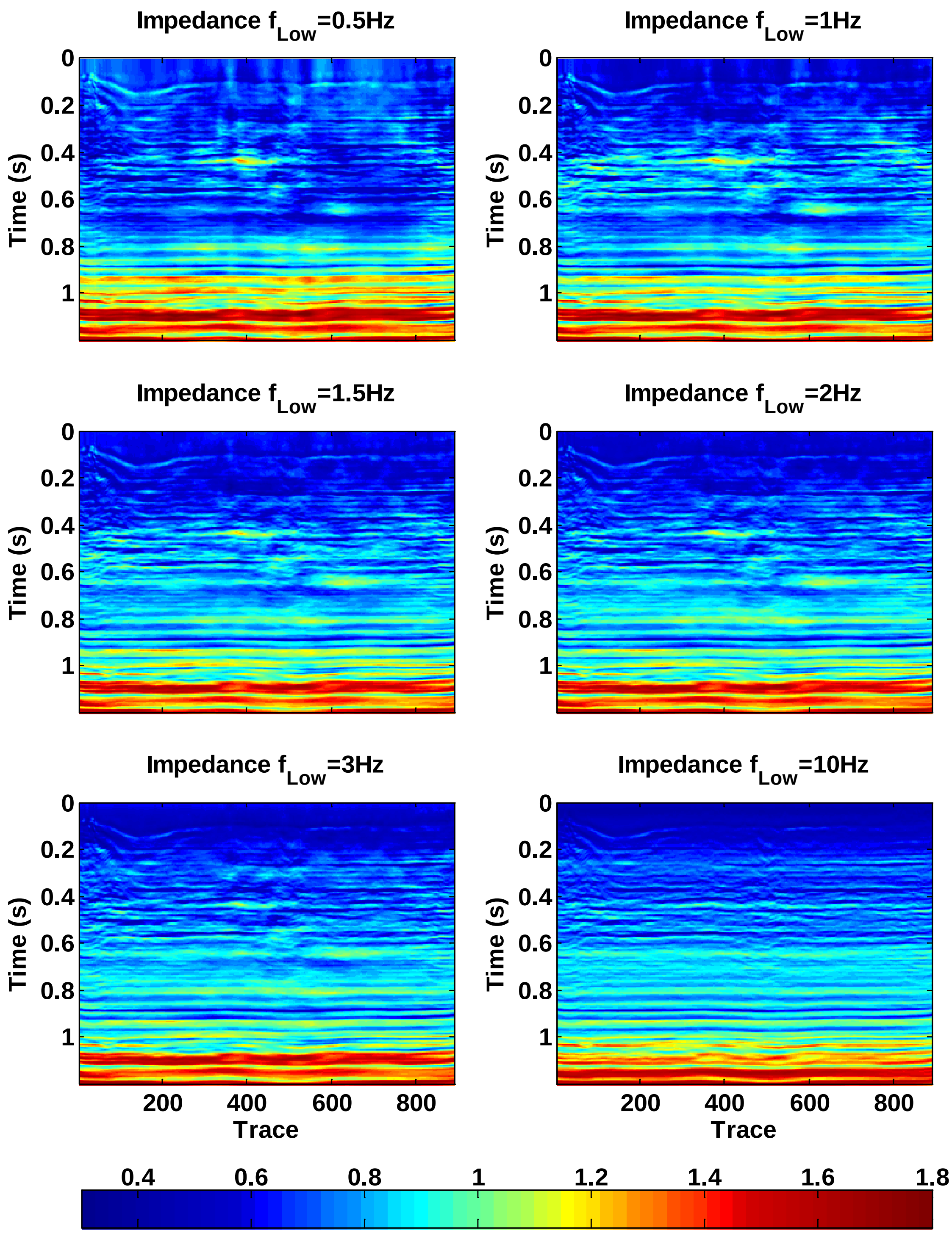


FIG 23: Impedance inversion sections using low-frequency cut-offs of 0.5, 1.0, 1.5, 2.0, 3.0 and 10.0 Hz

## CONCLUSIONS

The two most important things to consider when using BLIMP to compute an inversion are the low-frequency cut-off and the impedance log that is used. In this study we found that a low-frequency cut-off as low as 1.5 - 2 Hz could be used. Using the impedance log from well 12-27, the average error for three cross-validation tests was 11%. For the impedance log from well 14-27 the average cross-validation error was 10%, and the average cross-validation error for the impedance log from well 14-35 was 10%. While any of these well logs could be used to produce an adequate inversion the mean impedance of the three well logs produced the least amount of error during the cross-validation tests at 8.5%. This error is still slightly high; however the error in the reservoir interval (0.8 to 1 s) was only 6.5%. Most of the very high error is located where there is an overburden or underburden attached to the log with external information. This indicates that better choices for overburden and especially underburden are possible. These tests imply that for the 10Hz geophone, dynamite-source data there is reliable reflection signal down to 2 Hz and perhaps lower. Our inversions suggest that that the reflection signal band may extend down to 1.5 Hz with good confidence but signal quality becomes more spatially and temporally variable.

## REFERENCES

Ferguson, R. J. and Margrave, G. F., 1996, A simple algorithm for bandlimited impedance inversion: CREWES Research Report, Vol. 8, No. 21.

Isaac, J. H., Margrave, G. F., Deviat, M. and Nagarajappa, P., 2012, Processing and analysis of Hussar data for low frequency content: CREWES Research Report, Vol. 24.

Lindseth, R. O., 1979, Synthetic sonic logs – a process for stratigraphic interpretation: Geophysics, Vol. 44, No. 1.

Lloyd, H. J. E., and Margrave, G. F., 2012, Well tying and trace balancing Hussar data using new MATLAB tools: CREWES Research Report, Vol. 24.